



Quantifying the breakdown scale of pionless effective field theory

Downloaded from: <https://research.chalmers.se>, 2025-01-20 18:42 UTC

Citation for the original published paper (version of record):

Ekström, A., Platter, L. (2025). Quantifying the breakdown scale of pionless effective field theory. *Physics Letters, Section B: Nuclear, Elementary Particle and High-Energy Physics*, 860. <http://dx.doi.org/10.1016/j.physletb.2024.139207>

N.B. When citing this work, cite the original published paper.



Letter

Quantifying the breakdown scale of pionless effective field theory

Andreas Ekström^a, Lucas Platter^{b,c},^{*}^a Department of Physics, Chalmers University of Technology, SE-412 96, Göteborg, Sweden^b Department of Physics and Astronomy, University of Tennessee, Knoxville, TN 37996, USA^c Physics Division, Oak Ridge National Laboratory, Oak Ridge, TN 37831, USA

ARTICLE INFO

Editor: A. Schwenk

ABSTRACT

We use Bayesian statistics to infer the breakdown scale of pionless effective field theory in its standard power counting and with renormalization of observables carried out using the power-divergence subtraction scheme and cutoff regularization. We condition our inference on predictions of the total neutron-proton scattering cross section up next-to-next-to leading order. We quantify a median breakdown scale of approximately $1.4 m_\pi$. The 68% degree of belief interval is $[0.96, 1.69]m_\pi$. This result confirms the canonical expectation that the pion mass is a relevant scale in low-energy nuclear physics.

1. Introduction

Effective field theories (EFTs) [1] have emerged as important tools in nearly all areas of physics. They facilitate precise and systematic descriptions of observables without requiring a complete understanding of an underlying theory by focusing on the relevant degrees of freedom. A requirement for the applicability of an EFT is the existence of a sufficiently large separation of scales inherent to the system under study, as only then does the ratio of these scales provide a useful expansion parameter.

One type of EFT, the short-range EFT [2–4], has found wide application in particle, nuclear, and atomic physics. This non-relativistic EFT is built solely from contact interactions and is applicable when the two-body scattering length, a , is much larger than the range, R , of the interaction. In atomic physics, short-range EFT has been used to analyze three-body recombination in ultra-cold atomic gases and to relate its loss features to the Efimov effect [5]. In nuclear physics, it has been applied to describe a wide range of low-energy phenomena in the positive- and negative-energy spectra of light-mass nuclear systems [6]. Moreover, this type of EFT has enabled the calculation of electroweak processes in the two- and three-nucleon systems and served as a framework for describing electroweak processes involving halo nuclei, consisting of a few nucleons weakly bound to a tightly bound core [7]. In particle physics, contact EFT is a powerful tool to understand the properties of weakly bound mesonic molecules like the $X(3872)$ [8].

Given that EFTs offer a methodical order-by-order approach, they were heralded as providing reliable uncertainty estimates. To quantify these uncertainties—both from truncating the EFT expansion [9] and in parameter estimation [10]—Bayesian methods were developed. Recently, it has been recognized that Bayesian approaches can be used to quantify the breakdown scale, M_{hi} , of an EFT [11]. The breakdown scale crucially determines the momentum-scale for which the EFT is expected to fail, though it is not always straightforward to quantify. Indeed, until we have quantitative knowledge about the properties of the underlying theory, low-energy quantum chromodynamics in the case of nucleons, M_{hi} remains an inferred quantity rather than a precisely defined one. In the case of pionless EFT (the short-range EFT for nucleons), the canonical expectation for the breakdown scale is momenta corresponding to the pion mass, $m_\pi \approx 138$ MeV. This is because pion exchange—the longest-range nuclear interaction, as described by Yukawa [12]—is omitted from this EFT.

In this work, we use order-by-order predictions of the total neutron-proton scattering cross section to quantify M_{hi} and thereby also critically test the fundamental underpinnings of pionless EFT. During the preparation of this manuscript, we became aware of Ref. [13], which investigates the breakdown scale of a theory constructed solely from contact interactions in the context of nucleon-nucleon scattering. That work follows an ordering scheme for subleading interactions which differs from the approach typically used in pionless EFT. Consequently, its results are not directly comparable to our findings. The present work

* Corresponding author.

E-mail addresses: andreas.ekstrom@chalmers.se (A. Ekström), lplatter@utk.edu (L. Platter).<https://doi.org/10.1016/j.physletb.2024.139207>

Received 15 October 2024; Received in revised form 13 December 2024; Accepted 13 December 2024

highlights the strength of combining Bayesian methods with an order-by-order renormalizable EFT to leverage its inferential advantages.

2. Pionless EFT

This is a field theoretical formulation of effective range theory [14]. It uses a non-relativistic Lagrangian built from contact interactions only

$$\mathcal{L} = N^\dagger (i\partial_t + \frac{\nabla^2}{2m})N + \sum_{\alpha} \mathcal{L}_{\alpha} + \mathcal{L}_{sd}, \quad (1)$$

where N denotes the nucleon field and $\alpha = {}^1S_0, {}^3S_1$ are the spin-singlet (s) and spin-triplet (t) contributions to the S -wave two-nucleon scattering channel

$$\begin{aligned} \mathcal{L}_{\alpha} = & -C_0^{\alpha} (N^\dagger P_i^{\alpha} N)^\dagger (N^T P_i^{\alpha} N) \\ & + \frac{C_2^{\alpha}}{8} \left[(N^T P_i^{\alpha} N)^\dagger (N^T \bar{\nabla}^2 P_i^{\alpha} N) + \text{h.c.} \right], \end{aligned} \quad (2)$$

where C_0^{α} and C_2^{α} are low-energy coupling constants adjusted to the effective range parameters [15]. At next-to-next-to-leading order (N2LO), an S - to D -wave operator is formally required to calculate the scattering amplitude, denoted in Eq. (1) as \mathcal{L}_{sd} . However, it does not contribute to the total cross section up to N2LO.

We calibrate the coupling constants of this Lagrangian to reproduce the effective range parameters determined by the Nijmegen partial wave analysis [16,17]. To do this, we expand around the pole in the triplet channel

$$k \cot \delta_t = -\gamma_t + \frac{\rho_t}{2} (k^2 + \gamma_t^2) + \dots, \quad (3)$$

where k is the relative momentum between the two nucleons, $\gamma = \sqrt{mB_d}$ is the binding momentum associated with the binding energy B_d of the deuteron. In the singlet channel, we expand around the scattering threshold

$$k \cot \delta_s = -\frac{1}{a_s} + \frac{r_s}{2} k^2 + \dots \quad (4)$$

Pionless EFT requires a re-summation of the contact operators at leading order to reproduce the analytic structure of the S -matrix that generates the low-energy bound state (the deuteron) in the triplet channel and a virtual state in the singlet channel. The two-body spin-singlet t -matrix t_s containing the effective range parameters is therefore expanded in the small length scale r_s

$$\begin{aligned} t_s(k) = & \frac{1}{-\frac{1}{a_s} - ik} \left[1 - \frac{r_s}{2} k^2 \frac{1}{-\frac{1}{a_s} - ik} \right. \\ & \left. + \left(\frac{r_s}{2} k^2 \frac{1}{-\frac{1}{a_s} - ik} \right)^2 + \dots \right]. \end{aligned} \quad (5)$$

A similar expansion is carried out in the triplet channel for the triplet t -matrix t_t where (3) is used. The first term in the expansion in Eq. (5) is reproduced in the pionless EFT by summing all diagrams that contain only vertices arising from the first term in Eq. (2) and calibrating the low-energy constant $C_0^{1S_0}$ accordingly. The remaining terms are reproduced by including the subleading operators in Eq. (2) in perturbation theory. In this way, the low-energy constants become functions of the parameters in the effective range expansions [15]

$$a_s = -23.714 \text{ fm}, r_s = 2.678 \text{ fm}, \quad (6)$$

$$\gamma^{-1} = 4.318946 \text{ fm}, \rho_t = 1.765 \text{ fm}, \quad (7)$$

and we calculate the total cross section as

$$\sigma(k) = 4\pi \left(\frac{1}{4} |t_s(k)|^2 + \frac{3}{4} |t_t(k)|^2 \right). \quad (8)$$

The calculation of the scattering amplitude includes loop diagrams that are power-divergent. Therefore, a regularization scheme has to be employed before renormalization to the physical parameters in Eq. (6). The so-called power-divergence subtraction (pds) scheme [4] is a regularization approach that replaces any power divergence with a single power of the renormalization scale μ . After renormalization in the pds scheme, the on-shell two-nucleon t -matrix reproduces the effective range expansion up to the order of the EFT expansion exactly, i.e., it does not exhibit any residual regulator dependence. Alternatively, the loop integrals can employ a hard momentum space cutoff Λ . When this is done, the amplitude will display residual regulator dependence that is one order higher than the one considered. In this work, we primarily use pds regularization, but we also explore the effects of cutoff regularization on our inferences.¹

3. Inferring the breakdown scale

Having established the theoretical framework for pionless EFT, we now turn to the application of Bayesian inference to quantify the breakdown scale M_{hi} . We express the n -th order EFT prediction of the total cross σ section, at relative on-shell momentum k , as a series expansion, i.e., we formally write

$$\sigma^{(n)}(k) = \sigma_{\text{ref}}(k) \sum_{i=0}^n c_i(k) [Q(k)]^i. \quad (9)$$

The expected systematicity of pionless EFT manifests in the dimensionless ratio $Q(k) = f(k)/M_{\text{hi}}$ and an expectation of natural values for the EFT expansion coefficients c_i . We assume a functional form $f(k)$ that smoothly interpolates over the soft scale $\sim 1/a_t$, where $a_t = 5.42$ fm, as

$$f(k; r) = \frac{k^r + (1/a_t)^r}{k^{r-1} + (1/a_t)^{r-1}}, \quad r = 6 \quad (10)$$

This function is roughly constant for $ka_t < 1$ and smoothly matches to a linearly increasing function k/M_{hi} . In accordance with our expectation of naturally sized expansion coefficients c_i , i.e., $c_i \approx \mathcal{O}(1)$, we employ a normally distributed prior density²

$$c_i | \bar{c}^2 \stackrel{\text{iid}}{\sim} \mathcal{N}(0, \bar{c}^2) \quad (11)$$

$$\bar{c}^2 | \text{naturalness} \sim \chi^{-2}(\nu_0 = 2, \tau_0^2 = 1), \quad (12)$$

with a hyperprior for the variance \bar{c}^2 following an inverse χ^2 distribution with degrees of freedom $\nu_0 = 2$ and scale parameter $\tau_0 = 1$, equivalent to an inverse gamma distribution $\mathcal{IG}(a_0 = 1, b_0 = 1)$, see Fig. 1. For this choice of prior we have $\mathbb{P}(\bar{c}^2 \in [1/3, 3]) \approx 0.67$, i.e. a majority of the probability for the variance remains natural.

All dimensionful factors are collected in a reference scale σ_{ref} which renders the expansion coefficients c_i dimensionless. Our statistical analysis will be conditioned on leading order (LO, $n = 0$), next-to-leading order (NLO $n = 1$), and next-to-next-to-leading order (N2LO, $n = 2$) predictions for the total cross section at a finite number of momenta k . Information about the breakdown scale flows through the momentum-dependent order-by-order differences of predictions $\sigma^{(j)}$ and $\sigma^{(j-1)}$ via the corresponding expansion coefficients

$$c_j(k) = \frac{\sigma^{(j)}(k) - \sigma^{(j-1)}(k)}{\sigma_{\text{ref}} [Q(k)]^j}. \quad (13)$$

We utilize the leading-order pionless EFT prediction as the reference scale and therefore have that $c_0 = 1$. A collection of order-by-order predictions at K different momenta is denoted by a boldface symbol; σ . Up to N2LO, we can extract $N = 2$ informative coefficients $c_1(k)$ and $c_2(k)$

¹ See the supplemental material for more information on regularization and renormalization with a hard momentum space cutoff.

² The statistics notation $x \sim \cdot$ is shorthand for “ x is distributed as ...”. The abbreviation iid stands for independent and identically distributed.

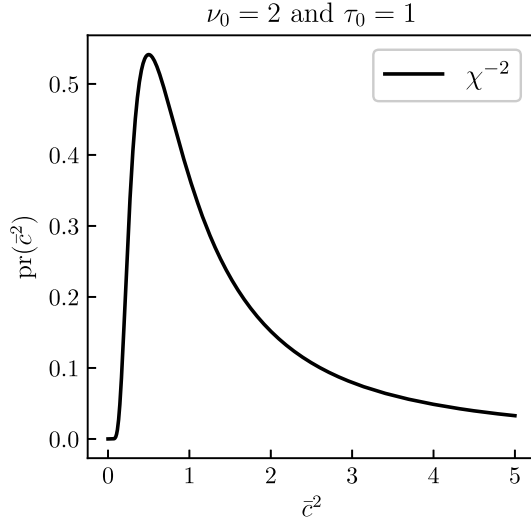


Fig. 1. Inverse- χ^2 prior for the variance of the normally distributed prior we place on the EFT expansion coefficients c_i defined in Eq. (9).

at momenta (k_1, k_2, \dots, k_K) . Using Bayes' rule, we express the posterior probability for M_{hi} , given σ and additional assumptions I , specified above and below, as

$$p(M_{\text{hi}}|\sigma, I) \propto p(\sigma|M_{\text{hi}}, I)p(M_{\text{hi}}|I). \quad (14)$$

To avoid overly correlated samples, which would contradict our iid assumption for the expansion coefficients, we computed cross sections at $K = 3$ different laboratory scattering energies (10, 40, and 70 MeV) corresponding to relative momenta $k = (68.5, 137.0, 181.2)$ MeV [18]. Below we analyze the robustness of our inference with respect to this choice of scattering energies.

The iid assumption enables a factorization of the data likelihood

$$p(\sigma|M_{\text{hi}}, I) = \prod_{i=1}^K p(\sigma_i|M_{\text{hi}}, I). \quad (15)$$

Following Melendez *et al.* [11] we can make a variable transformation and express the data likelihood at each momentum k_i as a joint distribution for the corresponding expansion coefficients. Moreover, having placed a (conjugate) inverse- χ^2 prior (with hyperparameters $\nu_0 = 2$, and $\tau_0 = 1$) on the expansion coefficients yields a closed form expression for $p(\sigma|M_{\text{hi}}, I)$. We thus have

$$p(M_{\text{hi}}|\sigma, I) \propto p(M_{\text{hi}}|I) \prod_{i=1}^K \left(\tau_i^{\nu_i} \prod_{n \in [1,2]} Q(k_i)^n \right)^{-1}, \quad (16)$$

where τ_i and ν_i are given by

$$\nu_i = \nu_0 + n_c, \quad (17)$$

and

$$\nu_i \tau_i^2 = \nu_0 \tau_0^2 + c_1(k_i)^2 + c_2(k_i)^2, \quad (18)$$

and $n_c = 2$ is the number of order-by-order differences $c_1(k_i)$ and $c_2(k_i)$ for each of the K momenta. The last step before we can evaluate the posterior for the breakdown scale is to express our prior $p(M_{\text{hi}}|I)$. To begin with, we adopt scale-invariant log-uniform distribution across a rather large interval of possible values $M_{\text{hi}} \in (m_\pi/40, 40m_\pi)$.

4. Results

We find posteriors at NLO and N2LO for the breakdown scale M_{hi} as shown in Fig. 2. The N2LO posterior is slightly more precise, as expected. Indeed, the NLO posterior is conditioned on less data as the inverse-

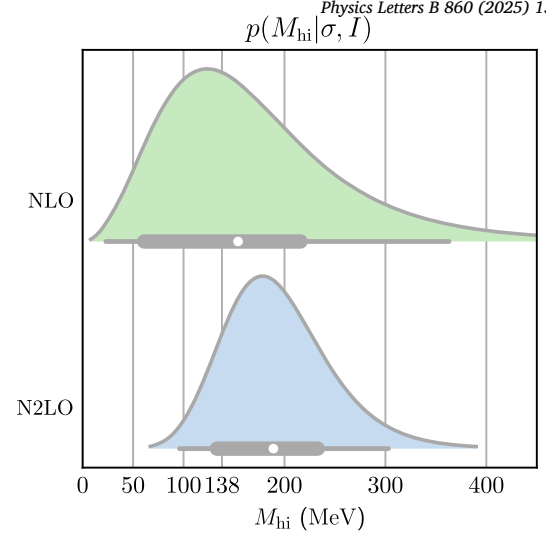


Fig. 2. Posteriors for the breakdown scale M_{hi} in pionless EFT. Thick and thin horizontal bars indicate 68% and 95% (highest posterior density) DoB intervals, respectively. The 68% (95%) DoB intervals are [61, 216] MeV ([23, 363] MeV) and [133, 233] MeV ([96, 303] MeV) at NLO and N2LO, respectively. The median values (white dots) for M_{hi} are 154 and 189 MeV at NLO and N2LO, respectively.

product over the orders in Eq. (16) is truncated at $n = 1$, which also modifies Eqs. (17)-(18) by $n_c = 1$ and $c_2(k_i) = 0$ for all k_i .

The inferred breakdown scale is consistent with the canonical scale separation that pionless EFT is predicated on. We find median values for M_{hi} at $1.1m_\pi$ and $1.4m_\pi$ at NLO and N2LO, respectively. Moreover, the order-by-order estimates of M_{hi} are consistent with each other as the NLO and N2LO posteriors overlap within the 68% degree of belief (dob) intervals. This is the main result of our work.

Our results are largely robust with respect to physically motivated variations of our prior assumptions. Modifying the prior for the EFT expansion parameters such that $\mathbb{P}(\bar{c}^2 \leq 1) = 0.62$ by setting $\nu_0 = 1$ and $\tau_0 = 1/2$, the posterior for M_{hi} is also shifted to somewhat lower values, and at N2LO we find a 68% DoB interval [80, 179] MeV and median $M_{\text{hi}} = m_\pi$. The NLO distribution sits at slightly lower values, as in the previous case. Regarding the soft-scale function $f(k; r)$ in Eq. (10), for $r > 6$ the resulting inference barely changes at all, as expected from the functional form of $f(k; r)$. However, for $r = 1$ we find median values of the breakdown scale at m_π for both NLO and N2LO. Using a uniform distribution for the prior $p(M_{\text{hi}}|I)$ across the interval $[m_\pi/2, 2m_\pi]$, we find median values $M_{\text{hi}} = 1.5m_\pi$ at both NLO and N2LO, with other characteristics of the distributions remaining largely unchanged. The median values for the breakdown scale are also robust with respect to the choice of scattering momenta at which we compute cross sections. Conditioning the inference on another choice of relative momenta, e.g., $k = 10, 80, 150$ MeV only serves to push the median breakdown scale up to $M_{\text{hi}} = 1.5m_\pi$ and $1.7m_\pi$ at NLO and N2LO, respectively. However, increasing the number of momentum values K can lead to artificially narrow posteriors, informed by correlated data, which violate the iid assumption underpinning our likelihood.

We inspect the pionless EFT predictions for the total cross section and quantify the corresponding truncation error up to N2LO, assuming $M_{\text{hi}} = 1.4m_\pi$ and the prior in Eqs. (11)-(12). The results are shown in Fig. 3. There is a clear trend of order-by-order improvement, and a rather good reproduction of experimental data up to $k = 50(100)$ MeV for NLO(N2LO). As a representative example, we also show the corresponding $c_1(k)$ and $c_2(k)$ EFT expansion coefficients in Fig. 4. The resulting expansion coefficients are of natural size, in agreement with our expectations. The resulting EFT truncation error is also reasonable, and we quantify this using a consistency plot, see Fig. 5. The procedure for computing a consistency plot of this kind is outlined in detail in Ref. [21]. In brief, we compare the coverage of the NLO truncation

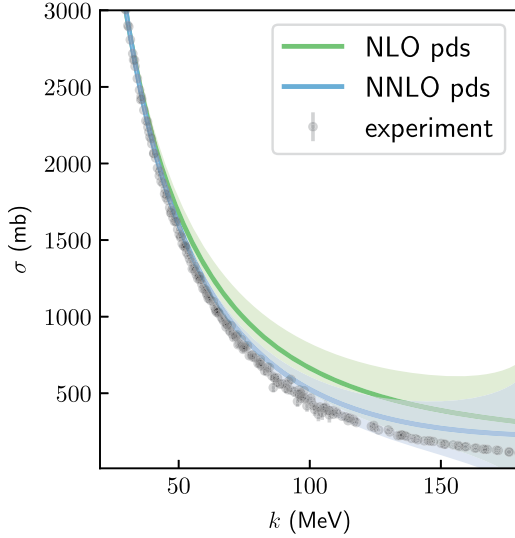


Fig. 3. Pionless EFT predictions for the total cross section at NLO and N2LO including 68% DoB intervals. Loop diagrams are regularized using pds, the coupling constants are calibrated to reproduce the effective range expansion, and we employ $M_{\text{hi}} = 1.4m_\pi$. Experimental cross section data is from the Granada database [19,20].

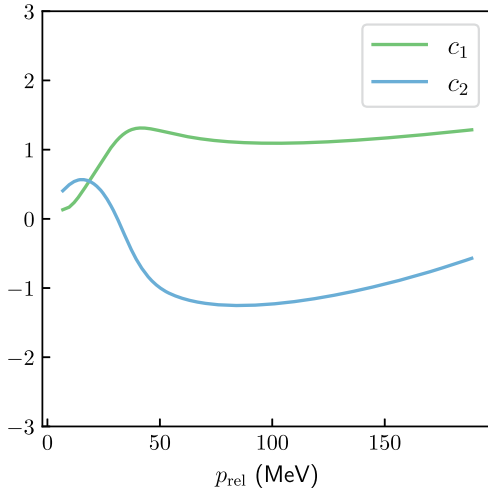


Fig. 4. EFT expansion coefficients c_1 and c_2 as extracted from the order-by-order predictions in Fig. 3.

error with the N2LO prediction, and we do so at 15 equally spaced lab scattering energies up to 75 MeV. The resulting NLO coverage is within the sampling error, assumed to follow a binomial distribution. For lower (higher) DoBs the NLO truncation error can be considered too small (large). This result is a further indication of a self-consistent and robust statistical analysis.

We carried out the same analysis for pionless EFT with cutoff regularization. We find that the inferred breakdown scale of $1.4m_\pi$ at NNLO is robust for regularization cutoff values $\gtrsim 1.5 \text{ fm}^{-1}$, while the NLO results show somewhat stronger variation with the cutoff. For lower values of the cutoff, the median value of the breakdown scale increases.

5. Summary

In this work, we inferred a median value $M_{\text{hi}} \approx 1.4 m_\pi$ for the breakdown scale of pionless EFT in pds regularization. Our statistical analysis is conditioned on order-by-order predictions for the total cross section up to N2LO. Our analysis is robust with respect to variations of our assumptions: natural expansion coefficients, iid cross section predictions,

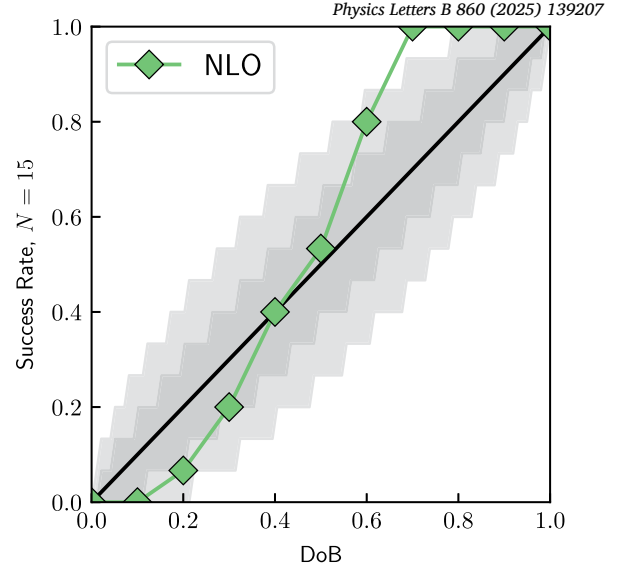


Fig. 5. Consistency plot for 15 NLO predictions at equally spaced lab scattering energies up to 75 MeV and varying DoB between 0% and 100%. The shaded bands represent 68% and 95% confidence intervals for the success rates.

and a log-uniform prior for M_{hi} . This result agrees with the canonical assumption that the pion sets the breakdown scale for an EFT that integrates out this mass scale in the nuclear interaction. However, it can also be considered somewhat large considering the pion cut at $m_\pi/2$ explicitly present in the S -wave projected one-pion exchange potential, see, e.g., Ref. [22] for one of many works relating the effective range expansion and its convergence radius to the pion cut. Therefore, further study of the breakdown scale at higher orders of the pionless EFT is warranted but will come at the cost of additional LECs. For instance, at third order—one order beyond what was considered here—the S -wave shape parameter and the P -wave scattering length enter the calculation of the total cross section. An operator leading to S to D wave mixing enters the calculation of the total cross section at the fourth order. However, this would also enable meaningful predictions of spin-polarized cross sections. Extension to pionless EFT analyses of neutron-deuteron scattering, where the renormalization of 3-nucleon observables up to N2LO is well understood and experimental data is abundant, should be straightforward.

The recent analysis by Bub *et al.* [13] examines a theory employing Weinberg power counting for the nuclear interaction while neglecting pion exchange contributions. As such, this approach consists solely of contact interactions, which superficially resembles pionless EFT. However, the underlying structure is markedly different. At order $(p/M_{\text{hi}})^4$ in their expansion scheme, with different scalings of the expansion parameter, Bub *et al.* consider a total of 26 low-energy constants and fit these to nucleon-nucleon scattering data. This has to be compared to the 6 low-energy constants used in our work, which are fitted to 4 experimental parameters. Bub *et al.* [13] infer, among many other model parameters, a posterior probability for the breakdown scale, obtaining typically $M_{\text{hi}} < 0.65m_\pi$, which is significantly lower than those in our analysis and expectations based on the excluded pion degree of freedom. They interpret this discrepancy as an indication of the importance of employing a consistent EFT power counting scheme and highlight the utility of a Bayesian approach for testing underlying assumptions.

Future work should address the inference sensitivity to calibrating the low-energy constants to cross-section data instead of the effective range parameters. The effective range parameters depend on the choice for the expansion of $k \cot \delta$ shown Eqs. (3) and (4). Direct calibration of the LECs to experimental data might deviate from these expansions and potentially influence the order-by-order improvement of EFT predictions. It would also be interesting to marginalize over such parametric uncertainties, as well as the uncertainty in M_{hi} [13].

As these developments in Bayesian parameter estimation and uncertainty quantification continue, they will not only enhance uncertainty quantification of pionless EFT calculations but also facilitate Bayesian model mixing of pionless EFT and pionful EFT [7,23,24]. Mixture EFTs, combining the strengths of both EFTs, might improve the inferences conditioned on these respective EFTs. This could, e.g., prove useful in cases like proton-proton fusion, where a unified and improved uncertainty estimate for the driving reaction rate in the Sun is desirable [25]. Finally, we remark that the approach we have used here can also be extended to the other areas where short-range EFT has been applied, provided some experimental data are available for model calibration. For example, inferring the breakdown scale of halo EFT would provide new insights into the physics of weakly bound nuclear systems.

Declaration of competing interest

The authors declare the following financial interests/personal relationships which may be considered as potential competing interests: Lucas Platter reports was provided by The University of Tennessee Knoxville. If there are other authors, they declare that they have no known competing financial interests or personal relationships that could have appeared to influence the work reported in this paper.

Acknowledgements

In this work, we used the Python package ‘gsum’ [11] to generate most of the plots. This work was supported by the Swedish Research Council (Grants No. 2020-05127), the National Science Foundation (Grant Nos. PHY-2111426 and PHY-2412612), and the US Department of Energy, Office of Nuclear Physics (Contract No. DE-AC05-00OR22725).

Appendix A. Supplementary material

Supplementary material related to this article can be found online at <https://doi.org/10.1016/j.physletb.2024.139207>.

Data availability

Data will be made available on request.

References

- [1] H. Georgi, *Effective field theory*, *Annu. Rev. Nucl. Part. Sci.* 43 (1993) 209.
- [2] U. van Kolck, *Effective field theory of short range forces*, *Nucl. Phys. A* 645 (1999) 273, arXiv:nucl-th/9808007.

- [3] D.B. Kaplan, M.J. Savage, M.B. Wise, *Two nucleon systems from effective field theory*, *Nucl. Phys. B* 534 (1998) 329, arXiv:nucl-th/9802075.
- [4] D.B. Kaplan, M.J. Savage, M.B. Wise, *A new expansion for nucleon-nucleon interactions*, *Phys. Lett. B* 424 (1998) 390, arXiv:nucl-th/9801034.
- [5] E. Braaten, H.W. Hammer, *Universality in few-body systems with large scattering length*, *Phys. Rep.* 428 (2006) 259, arXiv:cond-mat/0410417.
- [6] H.W. Hammer, S. König, U. van Kolck, *Nuclear effective field theory: status and perspectives*, *Rev. Mod. Phys.* 92 (2020) 025004, arXiv:1906.12122 [nucl-th].
- [7] H.W. Hammer, *Theory of halo nuclei*, in: I. Tanihata, H. Toki, T. Kajino (Eds.), *Handbook of Nuclear Physics*, 2022, pp. 1–30, arXiv:2203.13074 [nucl-th].
- [8] E. Braaten, M. Kusunoki, *Low-energy universality and the new charmonium resonance at 3870-MeV*, *Phys. Rev. D* 69 (2004) 074005, arXiv:hep-ph/0311147.
- [9] R.J. Furnstahl, N. Klco, D.R. Phillips, S. Wesolowski, *Quantifying truncation errors in effective field theory*, *Phys. Rev. C* 92 (2015) 024005, arXiv:1506.01343 [nucl-th].
- [10] I. Svensson, A. Ekström, C. Forssén, *Bayesian parameter estimation in chiral effective field theory using the Hamiltonian Monte Carlo method*, *Phys. Rev. C* 105 (2022) 014004, arXiv:2110.04011 [nucl-th].
- [11] J.A. Melendez, R.J. Furnstahl, D.R. Phillips, M.T. Prato, S. Wesolowski, *Quantifying correlated truncation errors in effective field theory*, *Phys. Rev. C* 100 (2019) 044001, arXiv:1904.10581 [nucl-th].
- [12] H. Yukawa, *On the interaction of elementary particles I*, *Proc. Phys. Math. Soc. Jpn.* 17 (1935) 48.
- [13] J.M. Bub, M. Piarulli, R.J. Furnstahl, S. Pastore, D.R. Phillips, *Bayesian analysis of nucleon-nucleon scattering data in pionless effective field theory*, arXiv:2408.02480 [nucl-th], 2024.
- [14] H.A. Bethe, *Theory of the effective range in nuclear scattering*, *Phys. Rev.* 76 (1949) 38.
- [15] J.-W. Chen, G. Rupak, M.J. Savage, *Nucleon-nucleon effective field theory without pions*, *Nucl. Phys. A* 653 (1999) 386, arXiv:nucl-th/9902056.
- [16] J.J. de Swart, C.P.F. Terheggen, V.G.J. Stoks, *The low-energy n p scattering parameters and the deuteron*, in: 3rd International Symposium on Dubna Deuteron 95, 1995, arXiv:nucl-th/9509032.
- [17] V.G.J. Stoks, R.A.M. Klomp, M.C.M. Rentmeester, J.J. de Swart, *Partial wave analysis of all nucleon-nucleon scattering data below 350-MeV*, *Phys. Rev. C* 48 (1993) 792.
- [18] I. Svensson, A. Ekström, C. Forssén, *Inference of the low-energy constants in Δ -full chiral effective field theory including a correlated truncation error*, *Phys. Rev. C* 109 (2024) 064003, arXiv:2304.02004 [nucl-th].
- [19] R. Navarro Pérez, J.E. Amaro, E. Ruiz Arriola, *Coarse-grained potential analysis of neutron-proton and proton-proton scattering below the pion production threshold*, *Phys. Rev. C* 88 (2013) 064002, Erratum: *Phys. Rev. C* 91 (2015) 029901, arXiv:1310.2536 [nucl-th].
- [20] R. Navarro Pérez, J.E. Amaro, E. Ruiz Arriola, *Partial wave analysis of nucleon-nucleon scattering below pion production threshold*, *Phys. Rev. C* 88 (2013) 024002, Erratum: *Phys. Rev. C* 88 (2013) 069902, arXiv:1304.0895 [nucl-th].
- [21] J.A. Melendez, S. Wesolowski, R.J. Furnstahl, *Bayesian truncation errors in chiral effective field theory: nucleon-nucleon observables*, *Phys. Rev. C* 96 (2017) 024003, arXiv:1704.03308 [nucl-th].
- [22] L. Mathelitsch, B.J. Verwest, *Effective range parameters in nucleon nucleon scattering*, *Phys. Rev. C* 29 (1984) 739.
- [23] E. Epelbaum, H.-W. Hammer, U.-G. Meissner, *Modern theory of nuclear forces*, *Rev. Mod. Phys.* 81 (2009) 1773, arXiv:0811.1338 [nucl-th].
- [24] R. Machleidt, D.R. Entem, *Chiral effective field theory and nuclear forces*, *Phys. Rep.* 503 (2011) 1, arXiv:1105.2919 [nucl-th].
- [25] B. Acharya, et al., *Solar fusion III: new data and theory for hydrogen-burning stars*, arXiv:2405.06470 [astro-ph.SR], 2024.